Probing the Ubiquinol-Binding Site in Cytochrome *bd* by Site-Directed Mutagenesis†

Tatsushi Mogi,*,‡,§,|| Satoru Akimoto,§ Sachiko Endou,§ Takahiro Watanabe-Nakayama,§ Eri Mizuochi-Asai,§ and Hideto Miyoshi⊥

Chemical Resources Laboratory, Tokyo Institute of Technology, Nagatsuta 4259, Midori-ku, Yokohama 226-8503, Japan, ATP System Project, Exploratory Research for Advanced Technology (ERATO), Japan Science and Technology Organization (JST), Nagatsuta, Midori-ku, Yokohama 226-0026, Japan, Department of Biological Sciences, Graduate School of Science, University of Tokyo, Hongo, Bunkyo-ku, Tokyo 113-0033, Japan, and Division of Applied Life Sciences, Graduate School of Agriculture, Kyoto University, Sakyo-ku, Kyoto 606-8502, Japan

Received January 30, 2006; Revised Manuscript Received April 6, 2006

ABSTRACT: To probe the structure of the quinol oxidation site in loop VI/VII of the *Escherichia coli* cytochrome *bd*, we substituted three conserved residues (Gln249, Lys252, and Glu257) in the N-terminal region and three glutamates (Glu278, Glu279, and Glu280) in the first internal repeat. We found that substitutions of Glu257 by Ala or Gln, and Glu279 and Glu280 by Gln, severely reduced the oxidase activity and the expression level of cytochrome *bd*. In contrast, Lys252 mutations reduced only the oxidase activity. Blue shifts in the 440 and 630 nm peaks of the reduced Lys252 mutants and in the 561 nm peak of the reduced Glu257 mutants indicate the proximity of Lys252 to the heme b_{595}-*d* binuclear center and Glu257 to heme b_{558}, respectively. Perturbations of reduced heme b_{558} upon binding of aurachin D support structural changes in the quinol-binding site of the mutants. Substitutions of Lys252 and Glu257 caused large changes in kinetic parameters for the ubiquinol-1 oxidation. These results indicate that Lys252 and Glu257 in the N-terminal region of the Q-loop are involved in the quinol oxidation by *bd*-type terminal oxidase.

Cytochrome *bd* is one of two terminal ubiquinol oxidases in the aerobic respiratory chain of *Escherichia coli* and is predominantly expressed under microaerophilic growth conditions (see refs *1*−*3* for reviews). It catalyzes dioxygen reduction with two molecules of ubiquinol-8, leading to the release of four protons from quinols to the periplasm. Through a putative proton channel, four protons used for dioxygen reduction are taken up from the cytoplasm and delivered to the dioxygen reduction site at the periplasmic side of the cytoplasmic membrane (*4*). During dioxygen reduction, cytochrome *bd* generates an electrochemical proton gradient across the membrane through apparent vectorial translocation of four chemical protons (*5*−*7*). In contrast to cytochrome *bo*, an alternative ubiquinol oxidase under highly aerated growth conditions, cytochrome *bd* has no proton pumping activity and does not belong to the heme−copper terminal oxidase superfamily.

Cytochrome *bd* has been isolated as a heterodimeric oxidase (CydAB, 100.6 kDa) and is distributed from Archaea to Eubacteria. Recent proteomic studies on the *E. coli* membrane proteins postulated YhcB (15 kDa) as a putative third subunit (*8*), but YhcB exists only in γ-Proteobacteria.[1] On the basis of spectroscopic and ligand binding studies, three distinct redox metal centers have been identified as heme b_{558}, heme b_{595}, and heme *d* (see ref *9* for a review). Unlike cytochrome *bo*, cytochrome *bd* does not contain a tightly bound ubiquinone-8. Heme b_{558} is a low-spin protoheme IX and is ligated by His186 (helix V) and Met393 (helix VII) of subunit I (CydA) (*10*) (Figure 1). Inhibitor binding studies indicate the close proximity of heme b_{558} to the quinol oxidation site (*12*, *13*). Heme b_{595} is a high-spin protoheme IX bound to His19 (helix I) of subunit I (*9*) and mediates electron transfer from heme b_{558} to heme *d* (*14*−*17*), where dioxygen is reduced to water. Heme *d* is a high-spin chlorin bound to an unidentified nitrogenous ligand (*18*−*20*) and forms a diheme binuclear center with heme b_{595} (*20*, *21*). Topological analysis suggests that all of the hemes are located at the periplasmic end of transmembrane helices (*4*).

In loop VI/VII (Q-loop) of subunit I, binding of monoclonal antibodies to ^{252}KLAAIEAEWET^{262} (*22*, 23) and proteolytic cleavage with trypsin at Tyr290 or chymotrypsin at Arg298 (*24*, *25*) suppressed ubiquinol oxidase activity (Figure 1). Yang et al. (*26*) reported the photoaffinity labeling of subunit I with 2-methyl-3-azido-5-methoxy-6-(3,7-dimethyl-[^{3}H]octyl)-1,4-benzoquinone. Recently, we synthesized 2-azido-3-methoxy- and 2-methoxy-3-azido-5-methyl-6-geranyl-1,4-

† This work was supported in part by JST (T.M., S.A., S.E., T.W.-N., and W.M.-A.) and Grant-in-Aid for Scientific Research from the Japan Society for the Promotion of Science (No. 15380083 to H.M.).

* To whom correspondence should be addressed at the Tokyo Institute of Technology. Tel: +81-45-922-5238. Fax: +81-45-922-5239. E-mail: tmogi@res.titech.ac.jp.

‡ Tokyo Institute of Technology.

§ Japan Science and Technology Organization.

|| University of Tokyo.

⊥ Kyoto University.

[1] We found recently that the Δ*yhcB* mutation did not affect the oxidase activity, heme binding, and subunit composition of cytochrome *bd* (T. Mogi et al., unpublished results).

10.1021/bi060192w CCC: $33.50
Published on Web 06/06/2006

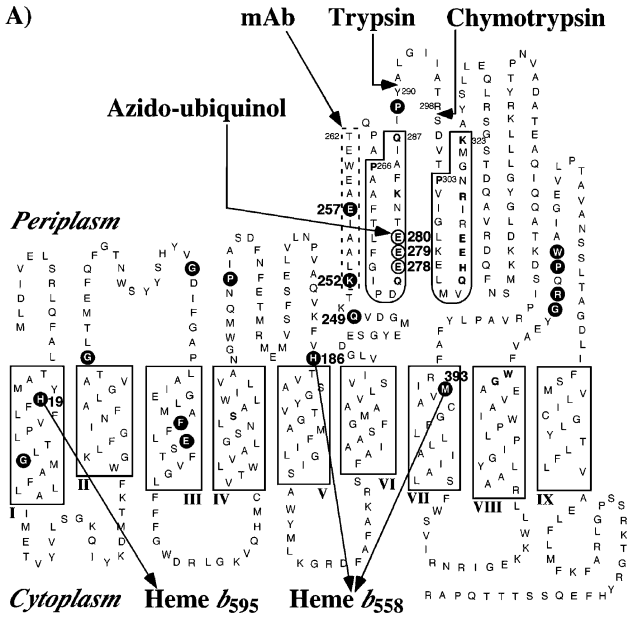

FIGURE 1: (A) Topological model of subunit I of the *E. coli* cytochrome *bd* (*4*) and (B) alignment of the N-terminal region of the Q-loop. (A) Amino acid substitutions were introduced at Gln249, Lys252, Glu257, Glu278, Glu279, and Glu280 in loop VI/VII. The epitope for mAb and putative internal repeats (Pro266−Gln287, Pro303−Lys323) are boxed. Strictly conserved residues are highlighted, and three glutamates in the first internal repeat are encircled. Proteolytic cleavage sites and the azidoubiquinol cross-linked site are indicated by arrows. His19 serves as the axial ligand for heme b_{595}, and His186 and Met393 serve as the axial ligand for heme b_{558}, which accepts electrons from quinols. (B) Amino acid sequences used for the alignment correspond to Gln249−Pro289 of *E. coli* subunit I (CydA), *E. coli* CydA (γ-Proteobacteria; U00096711), *Rhodobacter sphaeroides* (α-Proteobacteria; AF084032-1), *Bacillus subtilis* (Firmicutes; Z99123), *Chlorobium tepidum* (Chlorobi; AE012934), *Synechocystis* sp. PCC 6803 (Cyanobacteria; D90904), *Aquifex aeolicus* (Aquificae; AE000736), and *Halobacterium* sp. NRC-1 (Archaea; AE005171). The alignment was constructed by Clustal X (*11*). Conserved residues are shown in bold.

benzoquinone (*27*) and demonstrated the photoaffinity labeling of Glu280 of subunit I with azidoquinols (*28*). These findings suggest the presence of the ubiquinol oxidation site in loop VI/VII of subunit I that transfers electrons to heme b_{558} bound to the periplasmic ends of helices V and VII.

To probe the structure of the quinol oxidation site in Q-loop, we examined the effects of substitutions of three conserved residues (Gln249, Lys252, and Glu257) in the N-terminal region and three glutamates (Glu278, Glu279, and Glu280) in the first internal repeat (Figure 1). Characterization of mutant oxidases suggests that Lys252 and Glu257 in the N-terminal region of the Q-loop are involved in the quinol oxidation by cytochrome *bd*.

EXPERIMENTAL PROCEDURES

Mutagenesis and Expression of Cytochrome bd. Amino acid substitutions were introduced with QuickChange XL (Stratagene) using a pBR322 derivative pNG2 (*cyd*$^+$ Tet^R) (*29*) and synthetic oligonucleotides (Table S1). Ala substitution of Lys, Gln, and Glu residues would eliminate possible hydrophilic interactions, while Gln could substitute for Glu or Lys because of its size and hydrophilicity of the side chain. Mutations were confirmed by DNA sequencing (*30*).[2] For isolation of mutant enzymes, ST4683 (Δ*cyo*::Cm^R Δ*cyd*::Km^R) harboring a single copy plasmid pMFO9 (*cyo*$^+$ Amp^R) (*30*) was transformed with mutant pNG2 plasmids, and transformants were aerobically grown overnight in IM medium supplemented with 0.5% glucose, 12.5 μg/mL tetracycline, and trace metals (*31*). The yield of mutant cells from the 3 L culture was about 28 g wet weight.

Isolation of Mutant Cytochrome bd. Cells were suspended in 50 mM Tris-HCl (pH 7.4) containing 10 mM Na-EDTA, 1 mM phenylmethanesulfonyl fluoride (Sigma), and 0.5 mg/mL lysozyme (Sigma) and disrupted by two passages through a French pressure cell (Ohtake, Tokyo, Japan) at 1500 kg/cm^2. Cytoplasmic membrane vesicles were isolated by sucrose density centrifugation (*18*). Mutant enzymes were solubilized from membranes with 2.5% sucrose monolaurate (Mitsubishi-Kagaku Foods Co., Tokyo, Japan) and isolated by anion-exchange high-performance liquid chromatography on a TSKgel SuperQ-5PW column (21.5 mm i.d. × 15 cm; Tosoh), as described previously (*18*).[3] Purified enzymes in 50 mM sodium phosphate (pH 6.8) containing 0.1% sucrose monolaurate were stored at −80 °C until use.

Determination of Heme and Protein Content. Heme B content was determined by the pyridine ferrohemochromogen method, and heme D content was estimated from redox difference spectra using an extinction coefficient of $\epsilon_{628-651} = 27900$ (*32*). Protein concentration was determined by the BCA method (Pierce).

Absorption Spectroscopy. Absorption spectra of the air-oxidized and sodium hydrosulfite-reduced forms of mutant enzymes were determined with a V-550 UV/vis spectrophotometer (Jasco, Tokyo, Japan) at a final concentration of 5 [or 1.25 (I-E280A), 2.5 (I-E257A, I-E257Q, I-E279A, I-E279Q)] μM in 50 mM sodium phosphate (pH 7.4) containing 0.1% sucrose monolaurate. To probe structural changes in the quinol oxidation site near heme b_{558}, absolute spectra of the hydrosulfite-reduced mutant enzymes (2 μM) were measured in the presence of 10 μM aurachin D 5−10. Aurachin D 5−10 was synthesized by the previous method for aurachin C 3−11 and 4−11 (*33*).

Determination of Quinol Oxidase Activity. Quinol oxidase activity was determined at 25 °C by monitoring the absorbance change at 278 nm and calculated using an extinction coefficient of 12300 (*34*). The reaction mixture (1 mL) contained 50 mM sodium phosphate (pH 7.4), 0.1% sucrose monolaurate, and 12.5−125 nM purified cytochrome *bd*. The enzyme concentration was estimated from the heme B content, by assuming that cytochrome *bd* contains two *b*-hemes. The reaction was started by the addition of a reduced form of ubiquinone-1, a kind gift from Eisai Co. (Tokyo, Japan), at a final concentration of 400 μM. For

[2] Due to the presence of internal repeats in the *cydA* gene, we often found insertions in mutagenized plasmids.

[3] The introduction of the His_8 tag (Table S1) at the C-terminus of subunit I (CydA) severely reduced the expression level of cytochrome *bd*; thus the His-tag versions of the mutants were not used for the isolation of the enzyme.

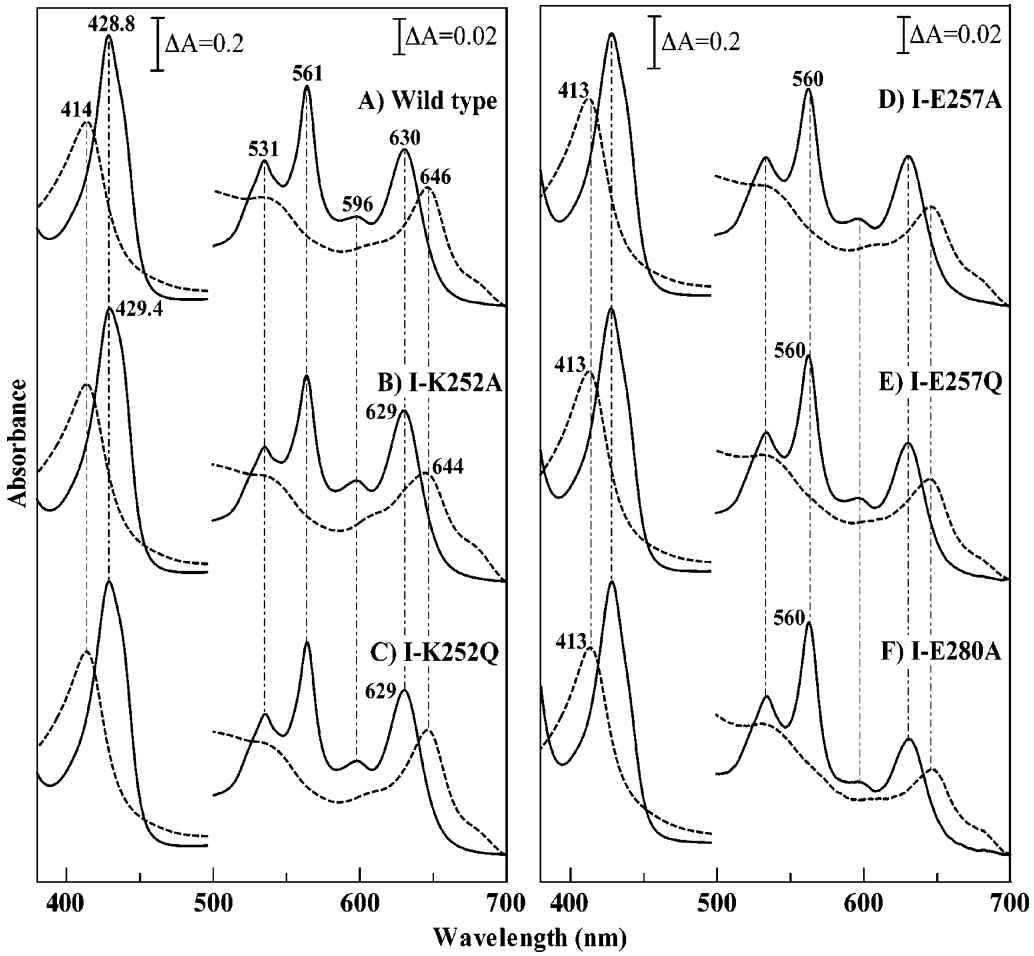

FIGURE 2: Absorption spectra of the air-oxidized (- - -) and fully reduced (—) forms of the Q-loop mutants of cytochrome *bd*. Absolute spectra of the isolated enzymes were recorded in 50 mM sodium phosphate (pH 7.4) containing 0.1% sucrose monolaurate before (- - -) and after reduction (—) with sodium hydrosulfite. The enzyme concentration was 5 [wild type (A), I-K252A (B), and I-K252Q (C)], 2.5 [I-E257A (D) and I-E257Q (E)], and 1.25 μM [I-E280A (F)]. The absorbance scale corresponds to the wild type.

kinetic analysis, the concentration of ubiquinol-1 was varied from 33 to 431 μM. K_m and V_{max} values were estimated with Kaleidagraph version 3.5 (Synergy Software).

RESULTS

Properties of Mutant Enzymes in Vivo and in Cytoplasmic Membranes. The in vivo activity of Q-loop mutants was examined by the aerobic complementation analysis using the terminal oxidase double deletion mutant ST4683, which cannot grow aerobically on a nonfermentable carbon source. In the minimal 0.5% glycerol medium, transformants with pNG2 carrying the I-E257A, I-E257Q, or I-E280Q mutation were unable to grow aerobically by oxidative phosphorylation (Table S2). The growth yield was decreased to two-thirds of the wild-type level in I-K252A and I-K252Q and to one-third in I-E279Q.

Effects of mutations on heme binding were studied in cytoplasmic membrane vesicles, which have been isolated from the cytochrome *bo*-expressing strain ST4683/pMFO9 ($\Delta cyo\ \Delta cyd/cyo^+$) harboring mutant pNG2. Heme *d* content showed that the expression level of mutant cytochrome *bd* was largely reduced in I-E257A, I-E257Q, I-E279Q, and I-E280Q (Table S2). The heme *d* to heme ($b + o$) ratios in other mutants indicate that over 90% of membrane-bound cytochrome was cytochrome *bd* (~25% of membrane proteins) under our growth conditions.

Ubiquinol-1 oxidase activity of mutant cytochrome *bd* in the membranes was determined in the presence of 2 mM KCN, which can completely suppress the quinol oxidase activity of cytochrome *bo* (K_i, 0.01 mM) (*5*). In addition to I-E257A, I-E257Q, I-E279Q, and I-E280Q mutants, I-K252A and I-K252Q mutants showed below 15% of the wild-type activity (Table S2). These results indicate that the I-Lys252 mutations reduced the oxidase activity and the I-Glu257, I-Glu279, and I-Glu280 mutations affected the oxidase activity and the expression level of mutant enzymes.

Effects of the Q-Loop Mutations on Spectroscopic Properties of Mutant Cytochrome bd. Absorption spectra of the air-oxidized and the fully reduced form of the isolated mutant enzymes were determined at room temperature. The 440 nm peak of ferrous heme b_{595} and the 630 nm peak of ferrous heme *d* showed a blue shift in I-K252A and I-K252Q, and the 646 nm peak of ferrous oxygenated heme *d* was shifted to 644 nm in I-K252A (Figure 2, Table S3). In contrast, the I-E257A, I-E257Q, and I-E280A mutations resulted in 1 nm blue shifts in the 414 nm peak of the air-oxidized enzyme and the 561 nm peak of ferrous heme b_{558}. Results indicate the proximity of Lys252 to the heme b_{595}-*d* binuclear center and Glu257 and Glu280 to heme b_{558}.

Effects of the Q-Loop Mutations on Binding of Aurachin D to Mutant Cytochrome bd. Aurachin D is one of specific inhibitors for cytochrome *bd* (*35*), and binding of decylau-

rachin D to the quinol oxidation site of the *Azotobacter* enzyme perturbs spectral properties and the redox potential of heme b_{558} (*13*). Binding of quinone to the Q_H site of *bo*-type oxidase results in similar effects on the electron-accepting heme *b* (*36*). To probe structural changes in the quinol oxidation site of the Q-loop mutants, we examined spectral changes of heme b_{558} induced by binding of aurachin D 5−10. Upon addition of aurachin D 5−10 to the hydrosulfite-reduced wild-type enzyme, we found similar red shifts in the α-band and Soret band regions (Figure 3A). The peak and trough in the (reduced *plus* inhibitor) *minus* reduced difference spectrum are 565 and 560 nm, respectively, for the α-band and 432.4 and 422 nm, respectively, in the Soret region (Figure 3B), comparable to 565 and 560 nm, respectively, and 432−433 and 423−424 nm, respectively, reported for the *Azotobacter* enzyme (*13*). In contrast, no spectral effects of aurachin D 5−10 on reduced heme b_{595} and reduced or oxygenated heme *d* were observed. In the Q-loop mutants, the I-K252A mutation eliminated such spectral shifts of heme b_{558} while the I-Q249A, I-E257A, and I-E280Q mutations decreased the amplitude of spectral changes and resulted in shifts in the peak and trough for the α-band and Soret band regions (Figure 3C−F). In addition, the 445 nm peak in I-Q249A suggests the perturbation of reduced heme b_{595}, and the 676 nm peak and 628 nm trough in I-E280Q indicates a partial conversion of ferrous heme *d* to oxoferryl heme *d*. In the wild type, 3 min incubation of the enzyme with 10 μM aurachin D 5−10 reduced the oxidase activity with 200 μM ubiquinol-1 to 8.9% of the control activity. We found that the residual activities of I-Q249A, I-K252A, I-E257A, and I-E280Q mutants were 31.5%, 30.5%, 94.5%, and 13.9%, respectively, indicating the resistance to the inhibitor. These findings support the proximity of the quinol- (and inhibitor) binding site to heme b_{558} and structural changes in the quinol oxidation site of these Q-loop mutant enzymes.

Effects of the Q-Loop Mutations on Kinetic Parameters for the Ubiquinol-1 Oxidation by Mutant Enzymes. At 100 μM ubiquinol-1, which is comparable to the K_m value of the wild-type enzyme, the oxidase activity of the I-K252A, I-K252Q, and I-E257A mutants was decreased to below 10% of the wild-type control and that of I-E257Q, I-E279Q, I-E280A, and I-E280Q to about one-third (Table S3).

In contrast to *bo*-type ubiquinol oxidase, the wild-type cytochrome *bd* exhibits the sigmoidal behavior of the oxidase activity against the concentration of ubiquinol-1 (*34*). By assuming the presence of the inactive population, such peculiar enzyme kinetics can be explained by the modified ping-pong bi-bi mechanism, where dioxygen reduction is tightly coupled to the sequential oxidation of two quinol molecules (*37*). The initial velocity for the ubiquinol-1 oxidation can be expressed as (*37*):

$$v = \frac{V_{max}[S]^2}{K_m{}^2 + K_m[S] + [S]^2} \quad (1)$$

The oxidation of ubiquinol-1 by the Q-loop mutants showed the sigmoidal dependence on the substrate concentration (Figure 4), and the kinetic parameters were estimated by eq 1 (Table 1). In I-K252A, I-K252Q, and I-E257A, the V_{max} value decreased to 5−31% of the wild-type control. The K_m value was estimated to be 93 μM in the wild type and increased 1.3−1.9-fold in I-Q249A, I-K252A, I-E278A, E278Q, and E279A, 2.6−3.1-fold in I-E257Q, I-E279Q, I-E279Q, I-E280A, and I-E280Q, and about 3.5-fold in I-K252Q and I-E257A. The K_m values (163−335 μM) of

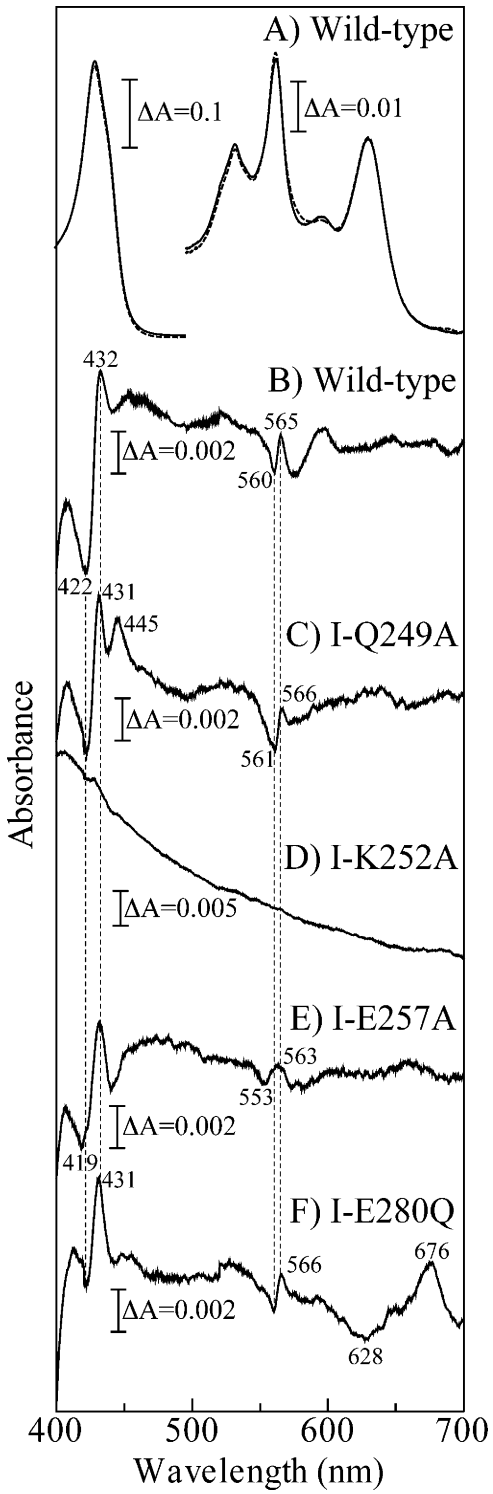

FIGURE 3: Spectral perturbations induced by binding of aurachin D 5−10 to the Q-loop mutants of cytochrome *bd*. (A) Absolute spectra of the reduced wild-type cytochrome *bd* (2 μM) in the absence (- - -) and presence (—) of 10 μM aurachin D 5−10 in 50 mM sodium phosphate (pH 7.4) containing 0.1% sucrose monolaurate. (B−F) (Reduced *plus* inhibitor) *minus* reduced difference spectra of the wild type (B), I-Q249A (C), I-K252A (D), I-E257A (E), and I-E280Q (F) mutants.

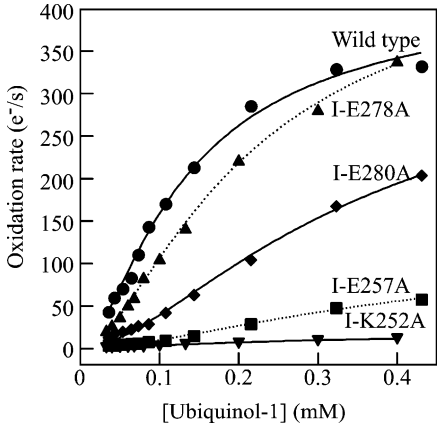

FIGURE 4: Dependence of ubiquinol oxidation by the Q-loop mutants on the ubiquinol-1 concentration. Data shown are wild type (●), I-K252A (▼), I-E257A (■), I-E278A (▲), and E280A (◆) mutants. Curve fitting was carried out with Kaleidagraph, and *R*-values are between 0.994 and 0.998 (0.996 average).

Table 1: Kinetic Parameters for Ubiquinol-1 Oxidation by Purified Q-Loop Mutants

mutant	K_m (μM)	V_{max} (e^-/s)	V_{max}/K_m (e^- s^{-1} μM^{-1})
wild type	93	438	4.71 (100)
I-Q249A	163	347	2.13 (45)
I-K252A	178	24	0.135 (2.9)
I-K252Q	335	54	0.161 (3.4)
I-E257A	323	135	0.418 (8.9)
I-E257Q	287	510	1.78 (38)
I-E278A	142	499	3.51 (75)
I-E278Q	139	418	3.01 (64)
I-E279A	124	417	3.36 (71)
I-E279Q	266	476	1.79 (38)
I-E280A	263	404	1.54 (33)
I-E280Q	243	434	1.79 (38)

cytochrome *bd* mutants are comparable to 242 μM of the K_m mutant (II-W136A) of cytochrome *bo* (*38*). A simultaneous change in the K_m and V_{max} values in I-K252A, I-K252Q, and I-E257A resulted in a large decrease in the V_{max} (k_{cat})/K_m ratio (only 3% of the wild-type control in I-K252A and I-K252Q and 9% in I-E257A). I-E257Q retained the V_{max} value at the wild-type level, indicating that Gln can partly substitute the role of Glu257. Results indicate that mutations at Gln249, Glu278, Glu279, and Glu280 perturbed the quinol oxidation site and that Lys252 and Glu257, which are conserved in cytochrome *bd*, are involved in the quinol oxidation.

DISCUSSION

Quinol Oxidation Site in Cytochrome bd. Cytochrome *bd*-type quinol oxidase is widely distributed from Archaea to Eubacteria and can use ubiquinol, plastoquinol, or menaquinol as electron donors. Steady-state kinetics of the quinol oxidation (*5*, *37*) and inhibitor binding studies (*13*) indicate the presence of a single quinol oxidation site in cytochrome *bd*. Binding of mAb to ^{252}KLAAIEAEWET^{262} in the Q-loop of subunit I inhibits the quinol oxidase activity (*22*, *23*) and may perturb the quinol oxidation site. Photoaffinity labeling studies with azidoquinols demonstrated the proximity of Glu280 in the Q-loop to the 2- and 3-methoxy groups on the ubiquinone ring (*28*). Although Glu280 is not conserved even in γ-Proteobacteria, the presence of Glu or Asp at ~10 amino acid residues upstream of the conserved Pro289 indicates the catalytic and/or structural role of acidic residue(s) in the binding pocket for methoxy groups of ubiquinone (Figure 1B). A loss of the quinol oxidase activity by proteolytic cleavages at either Tyr290 or Arg298 in the Q-loop (*24*, *25*) may be related to alterations in interactions of the first internal repeat (^{266}Px$_{10}$QEEEx$_2$Kx$_3$Q^{287}) with the second repeat (^{303}Px$_9$QHEEx$_2$Rx$_3$K^{323}) (Figure 1A). A hydrophilic segment containing Glu280 can be predicted to be a coil [P275−T281 by Jpred (*39*), I274−E280 by PROF (*40*), and G273−N282 by New Joint method (*41*)] between two short β-strands. Such a flexible structure would allow the accommodation of both a methoxy and a bulky rodlike azido group on the quinone ring and may be the molecular basis of wide substrate specificity of cytochrome *bd* (i.e., the use of ubiquinol-8 under aerobic growth conditions and menaquinol-8 under microaerophilic growth conditions in *E. coli*).

Mutagenesis studies on the N-terminal region of the Q-loop revealed that Lys252 and Glu257 are involved in the quinol oxidation. Conserved Lys252 and Glu257 in a putative short α-helix may serve as direct ligands and electron acceptors for the C_1-OH and/or C_4-OH groups of ubiquinol. Effects of the mutations on the heme binding suggest the orientation of the hydrophilic helix relative to hemes b_{558} and b_{595} in the transmembrane helices (i.e., the proximity of Glu257 and Lys252 to heme b_{558} and the heme b_{595}-*d* binuclear center, respectively). Electrons could be transferred from quinols to the propionate group(s) of heme b_{558} through Glu257 and a possible hydrogen bond network.

Substitutions of Gln249, Glu278, Glu279, and Glu280 resulted in a 1.3−2.9-fold increase in the K_m value for ubiquinol-1 (Table 1). The Ala mutation at Gln249, which is strictly conserved in cytochrome *bd*, perturbed the aurachin D-induced spectral changes (Figure 3) and increased 3.5-fold the resistance to aurachin D. Mutations at Glu280, which has been identified as a part of the binding pocket for the methoxy groups on the ubiquinone ring (*28*), caused the blue shift in the 561 nm peak of ferrous heme b_{558} and perturbed the aurachin D-induced spectral changes (Figures 2 and 3). These findings indicate that the proximity of Gln249 and Glu278-Glu279-Glu280 to the quinol oxidation site. It is also possible that, as found for the proteolytic cleavages of the Q-loop (*24*, *25*), structural perturbations induced by the mutations could affect the oxidase activity and the expression level.

Structures of Quinone Redox Sites in Respiratory Complexes. X-ray structures for *bo*-type ubiquinol oxidase (*42*), the cytochrome bc_1 complex (*43*−*46*), succinate dehydrogenase (*47*), fumarate reductase (*48*, *49*), nitrate reductase A (*50*), and formate dehydrogenase N (*51*) have been recently determined, but it appears that there is no common motif for the quinone/quinol binding. Due to low binding affinity, bound substrates were absent in the quinol oxidation site of *bo*-type ubiquinol oxidase (Q_L), the cytochrome bc_1 complex (Q_o), and nitrate reductase A. In the *E. coli bo*-type ubiquinol oxidase, mutagenesis (*38*, *52*) and photoaffinity labeling studies with azidoquinone (*53*) indicated that subunit II provides a part of the quinol oxidation site (Q_L). Further, mutagenesis and spectroscopic studies revealed the structure of the quinone-binding site (Q_H), which mediates electron transfer from the Q_L site to heme *b* (*42*, *54*, *55*).

In conclusion, photoaffinity-labeling studies with azidoquinols (*28*) and present site-directed mutagenesis studies

on the Q-loop revealed the structural features of the quinol oxidation site in cytochrome *bd*. X-ray crystallographic studies would provide further insights into the understanding of the catalytic mechanism for the quinol oxidation by *bd*-type terminal oxidase.

ACKNOWLEDGMENT

We thank R. B. Gennis (University of Illinois) for the *E. coli* strain GR84N/pNG2 and Eisai Co. (Tokyo, Japan) for ubiquinone-1.

SUPPORTING INFORMATION AVAILABLE

Table S1 showing the oligonucleotides used for site-directed mutagenesis, Table S2 summarizing the in vivo activity of the mutants and heme content and quinol oxidase activity of mutant membranes, and Table S3 providing a summary of oxidase activity, heme content, and spectroscopic properties of isolated mutant enzymes. This material is available free of charge via the Internet at http://pubs.acs.org.

REFERENCES

1. Ingledew, W. J., and Poole, R. K. (1984) The respiratory chain of *Escherichia coli*, *Microbiol. Rev. 48*, 222−271.
2. Jünemann, S. (1997) Cytochrome *bd* terminal oxidase, *Biochim. Biophys. Acta 1321*, 107−127.
3. Mogi, T., Tsubaki, M., Hori, H., Miyoshi, H., Nakamura, H., and Anraku, Y. (1998) Two terminal quinol oxidase families in *Escherichia coli*: Variations on molecular machinery for dioxygen reduction, *J. Biochem. Mol. Biol. Biophys. 2*, 79−110.
4. Zhang, J., Barquera, B., and Gennis, R. B. (2004) Gene fusions with β-lactamase show that subunit I of the cytochrome *bd* quinol oxidase from *E. coli* has nine transmembrane helices with the O_2 reactive site near the periplasmic surface, *FEBS Lett. 561*, 58−62.
5. Kita, K., Konishi, K., and Anraku, Y. (1984) Terminal oxidases of *Escherichia coli* aerobic respiratory chain. II. Purification and properties of cytochrome b_{558}-*d* complex from cells grown with limited oxygen and evidence of branched electron-carrying systems, *J. Biol. Chem. 259*, 3375−3381.
6. Miller, M. J., and Gennis, R. B. (1985) The cytochrome *d* complex is a coupling site in the aerobic respiratory chain of *Escherichia coli*, *J. Biol. Chem. 260*, 14003−14008.
7. Jasaitis, A., Borisov, V. B., Belevich, N. P., Morgan, J. E., Konstantinov, A. A., and Verkohsky, M. I. (2000) Electrogenic reactions of cytochrome *bd*, *Biochemistry 39*, 13800−13809.
8. Stenberg, F., Chovanec, P., Maslen, S. L., Robinson, C. V., Ilag, L. L., von Heijne, G., and Daley, D. O. (2005) Protein complexes of the *Escherichia coli* cell envelope, *J. Biol. Chem. 280*, 34409−34419.
9. Tsubaki, M., Hori, H., and T. Mogi (2000) Probing molecular structure of dioxygen reduction site of bacterial quinol oxidases through ligand binding to the redox metal centers, *J. Inorg. Biochem. 82*, 19−25.
10. Fang, G. H., Lin, R. J., and Gennis, R. B. (1989) Location of heme axial ligands in the cytochrome *d* terminal oxidase complex of *Escherichia coli* determined by site-directed mutagenesis, *J. Biol. Chem. 264*, 8026−8032.
11. Thompson, J. D., Gibson, T. J., Plewniak, F., Jeanmougin, F., and Higgins, D. G. (1997) The CLUSTAL_X windows interface: flexible strategies for multiple sequence alignment aided by quality analysis tools, *Nucleic Acids Res. 24*, 4876−4882.
12. Jünemann, S., and Wrigglesworth, J. M. (1994) Antimycin inhibition of the cytochrome *bd* complex from *Azotobacter vinelandii* indicates the presence of a branched electron transfer pathway for the oxidation of ubiquinol, *FEBS Lett. 345*, 198−202.
13. Jünemann, S., Wrigglesworth, J. M., and Rich, P. R. (1997) Effects of decyl-aurachin D and reversed electron transfer in cytochrome *bd*, *Biochemistry 36*, 9323−9331.
14. Poole, R. K., and Williams, H. D. (1987) Proposal that the function of the membrane-bound cytochrome a_1-like haemoprotein (cytochrome *b*-595) in *Escherichia coli* is a direct electron donation to cytochrome *d*, *FEBS Lett. 217*, 49−52.
15. Hill, B. C., Hill, J. J., and Gennis, R. B. (1994) The room temperature reaction of carbon monoxide and oxygen with the cytochrome *bd* quinol oxidase from *Escherichia coli*, *Biochemistry 33*, 15110−15115.
16. Kobayashi, K., Tagawa, S., and Mogi, T. (1999) Pulse radiolysis studies on electron transfer processes in cytochrome *bd*-type ubiquinol oxidase from *Escherichia coli*, *Biochemistry 38*, 5913−5917.
17. Zhang, J., Hellwig, P., Osborne, J. P., Huang, H., Moenne-Loccoz, P., Konstantinov, A. A., and Gennis, R. B. (2001) Site-directed mutation of the highly conserved region near the Q-loop of the cytochrome *bd* quinol oxidase from *Escherichia coli* specifically perturbs heme b_{595}, *Biochemistry 40*, 8548−8556.
18. Hirota, S., Mogi, T., Ogura, T., Anraku, Y., Gennis, R. B., and Kitagawa, T. (1995) Resonance Raman study on axial ligands of heme irons in cytochrome *bd*-type ubiquinol oxidase from *Escherichia coli*, *Biospectroscopy 1*, 305−311.
19. Sun, J., Kahlow, M. A., Kaysser, T. M., Osborne, J., Hill, J. J., Rohlfs, R. J., Hille, R., Gennis, R. B., and Loehr, T. M. (1996) Resonance Raman spectroscopic identification of a histidine ligand of b_{595} and the nature of the ligation of chlorin *d* in the fully reduced *Escherichia coli* cytochrome *bd* oxidase, *Biochemistry 35*, 2403−2412.
20. Hori, H., Tsubaki, M., Mogi, T., and Anraku, Y. (1996) EPR study of NO complex of *bd*-type ubiquinol oxidase from *Escherichia coli*. The proximal ligand of heme *d* is a nitrogenous amino acid residue, *J. Biol. Chem. 271*, 9254−9258.
21. Hill, J. J., Alben, J. O., and Gennis, R. B. (1993) Spectroscopic evidence for a heme-heme binuclear center in the cytochrome *bd* ubiquinol oxidase from *Escherichia coli*, *Proc. Natl. Acad. Sci. U.S.A. 90*, 5863−5867.
22. Kranz, R. G., and Gennis, R. B. (1984) Characterization of the cytochrome *d* terminal oxidase complex of *Escherichia coli* using polyclonal and monoclonal antibodies, *J. Biol. Chem. 259*, 7998−8003.
23. Dueweke, T. J., and Gennis, R. B. (1990) Epitopes of monoclonal antibodies which inhibit ubiquinol oxidase activity of *Escherichia coli* cytochrome *d* complex localize functional domain, *J. Biol. Chem. 265*, 4273−4277.
24. Lorence, R. M., Carter, K., Gennis, R. B., Matsushita, K., and Kaback, H. R. (1988) Trypsin proteolysis of the cytochrome *d* complex of *Escherichia coli* selectively inhibits ubiquinol oxidase activity while not affecting *N*,*N*,*N*′,*N*′-tetramethyl-*p*-phenylenediamine oxidase activity, *J. Biol. Chem. 263*, 5271−5276.
25. Dueweke, T. J., and Gennis, R. B. (1991) Proteolysis of the cytochrome *d* complex with trypsin and chymotrypsin localizes a quinol oxidase domain, *Biochemistry 30*, 3401−3406.
26. Yang, F. D., Yu, L., Yu, C. A., Lorence, R. M., and Gennis, R. B. (1986) Use of an azido-ubiquinone derivative to identify subunit I as the ubiquinol binding site of the cytochrome *d* terminal oxidase complex of *Escherichia coli*, *J. Biol. Chem. 261*, 14987−14990.
27. Sakamoto, K., Nomura, K., and Miyoshi, H. (2002) Synthesis and electron-transfer activity of azido ubiquinone-2, *J. Pestic. Sci. 27*, 147−149.
28. Matsumoto, Y., Murai, M., Fujita, D., Sakamoto, K., Miyoshi, H., Yoshida, M., and Mogi, T. (2006) Mass spectrometric analysis of the ubiquinol-binding site in cytochrome *bd* from *Escherichia coli*, *J. Biol. Chem. 281*, 1905−1912.
29. Green, G. N., Kranz, R. G., Lorence, R. M., and Gennis, R. B. (1984) Identification of subunit I as the cytochrome b_{558} component of the cytochrome *d* terminal oxidase complex of *Escherichia coli*, *J. Biol. Chem. 259*, 7994−7997.
30. Mogi, T., Minagawa, J., Hirano, T., Sato-Watanabe, M., Tsubaki, M., Uno, T., Hori, H., Nakamura, H., Nishimura, Y., and Anraku, Y. (1998) Substitutions of conserved aromatic amino acid residues in subunit I perturb the metal centers of the *Escherichia coli bo*-type ubiquinol oxidase, *Biochemistry 37*, 1632−1639.
31. Kandori, H., Nakamura, H., Yamazaki, Y., and Mogi, T. (2005) Redox-induced protein structural changes in cytochrome *bo* revealed by Fourier transform infrared spectroscopy and ^{13}C-Tyr-labeling, *J. Biol. Chem. 280*, 32821−32826.
32. Tsubaki, M., Hori, H., Mogi, T., and Anraku, Y. (1995) Cyanide-binding site of *bd*-type ubiquinol oxidase from *Escherichia coli*, *J. Biol. Chem. 270*, 28565−28569.
33. Miyoshi, H., Takegami, K., Sakamoto, K., Mogi, T., and Iwamura, H. (1999) Characterization of the ubiquinol oxidation sites in

cytochromes *bo* and *bd* from *Escherichia coli* using aurachin C analogues, *J. Biochem. 125*, 138−142.
34. Sakamoto, K., Miyoshi, H., Takegami, K., Mogi, T., Anraku, Y., and Iwamura, H. (1996) Probing substrate binding site of the *Escherichia coli* quinol oxidases using synthetic ubiquinol analogues based upon their electron-donating efficiency, *J. Biol. Chem. 271*, 29897−29902.
35. Meunier, B., Madgwick, S. A., Reil, E., Oettmeier, W., and Rich, P. R. (1995) New inhibitors of the quinol oxidation sites of bacterial cytochromes *bo* and *bd*, *Biochemistry 34*, 1076−1083.
36. Sato-Watanabe, M., Itoh, S., Mogi, T., Matsuura, K., Miyoshi, H., and Anraku, Y. (1995) Stabilization of a semiquinone radical at the high affinity quinone binding site of the *Escherichia coli bo*-type ubiquinol oxidase, *FEBS Lett. 374*, 265−269.
37. Matsumoto, Y., Muneyuki, E., Fujita, D., Sakamoto, K., Miyoshi, H., Yoshida, M., and Mogi, T. (2006) Kinetic mechanism of quinol oxidation by cytochrome *bd* studied with ubiquinone-2 analogs, *J. Biochem. 139*, 779−788.
38. Ma, J., Puustinen, A., Wikström, M., and Gennis, R. B. (1998) Tryptophan-136 in subunit II of cytochrome bo_3 from *Escherichia coli* may participate in the binding of ubiquinol, *Biochemistry 37*, 11806−11811.
39. Cuff, J. A., Clamp, M. E., Siddiqui, A. S., Finlay, M., and Barton, G. J. (1998) JPred: a consensus secondary structure prediction server, *Bioinformatics 14*, 892−893.
40. Ouali, M., and King, R. D. (2000) Cascaded multiple classifiers for secondary structure prediction, *Protein Sci. 9*, 1162−1176.
41. Ito, M., Matsuo, Y., and Nishikawa, K. (1997) Prediction of protein secondary structure using the 3D-1D compatibility algorithm, *Comput. Appl. Biosci. 13*, 415−424.
42. Abramson, J., Riistama, S., Larsson, G., Jasaitis, A., Svensson-Ek, M., Laakkonen, L., Puustinen, A., Iwata, S., and Wikström, M. (2000) The structure of the ubiquinol oxidase from *Escherichia coli* and its ubiquinone binding site, *Nat. Struct. Biol. 7*, 910−917.
43. Xia, D., Yu, C.-A., Kim, H., Xia, J.-Z., Kachurin, A. M., Zhang, L., Yu, L., and Deisenhofer, J. (1997) Crystal structure of the cytochrome bc_1 complex from bovine heart mitochondria, *Science 277*, 60−66.
44. Zhang, Z., Huang, L., Shulmeister, V. M., Chi, Y.-I., Kim, K. K., Hung, L.-W., Crofts, A. R., Berry, E. A., and Kim, S.-H. (1998) Electron transfer by domain movement in cytochrome bc_1, *Nature 392*, 677−684.
45. Iwata, S., Lee, J. W., Okada, K., Lee, J. K., Iwata, M., Rasmussen, B., Link, T. A., Ramaswamy, S., and Jap, B. K. (1998) Complete structure of the 11-subunit bovine mitochondrial cytochrome bc_1 complex, *Science 281*, 64−71.
46. Palsdottir, H., Lojero, C. G., Trumpower, B. L., and Hunte, C. (2003) Structure of the yeast cytochrome bc_1 complex with a hydroxyquinone anion Q_o site inhibitor bound, *J. Biol. Chem. 278*, 31303−31311.
47. Yankovskaya, V., Horsefield, R., Törnroth, S., Luna-Chavez, C., Miyoshi, H., Léger, C., Byrne, B., Cecchini, G., and Iwata, S. (2003) Architecture of succinate dehydrogenase and reactive oxygen species generation, *Science 299*, 700−704.
48. Iverson, T. M., Luna-Chavez, C., Cecchini, G., and Rees, D. C. (1999) Structure of the *Escherichia coli* fumarate reductase respiratory complex, *Science 284*, 1961−1966.
49. Lancaster, C. R. D., Kröger, A., Auer, M., and Michel, H. (199) Structure of fumarate reductase from *Wolinella succinogenes* at 2.2 Å resolution, *Nature*, 377−385.
50. Bertero, M., Rothery, R., Palak, M., Hou, C., Lim, D., Blasco, F., Weiner, J. H., and Strynadka, N. C. J. (2003) Insights into the respiratory electron transfer pathway from the structure of nitrate reductase A, *Nat. Struct. Biol. 10*, 681−687.
51. Jormakka, M., Törnroth, S., Byrne, B., and Iwata, S. (2002) Molecular basis of proton motive force generation: Structure of formate dehydrogenase-N, *Science 295*, 1863−1868.
52. Sato-Watanabe, M., Mogi, T., Miyoshi, H., and Anraku, Y. (1998) Isolation and characterizations of quinone analogue-resistant mutants of *bo*-type ubiquinol oxidase from *Escherichia coli*, *Biochemistry 37*, 12744−12752.
53. Tsatsos, P. H., Reynolds, K., Nickels, E. F., He, D.-Y., Yu, C.-A., and Gennis, R. B. (1998) Using matrix-assisted laser desorption ionization mass spectrometry to map the quinol binding site of cytochrome bo_3 from *Escherichia coli*, *Biochemistry 37*, 9884−9888.
54. Hellwig, P., Barquera, B., and Gennis, R. B. (2001) Direct evidence for the protonation of aspartate-75, proposed to be at a quinol binding site, upon reduction of cytochrome bo_3 from *Escherichia coli*, *Biochemistry 40*, 1077−1082.
55. Grimaldi, S., Ostermann, T., Weiden, N., Mogi, T., Miyoshi, H., Ludwig, B., Michel, H., Prisner, T. F., and MacMillan, F. (2003) Asymmetric binding of the high-affinity $Q_H^{\bullet-}$ ubisemiquinone in quinol oxidase (bo_3) from *Escherichia coli* studied by multifrequency electron paramagnetic resonance spectroscopy, *Biochemistry 42*, 5632−5639.

BI060192W